

Technical Report Documentation Page

1. Report No. LS-23-RP-01	2. Government Accession No. N/A	3. Recipient's Catalog No. N/A	
4. Title and Subtitle Design, Manufacturing, and Characterization of Fiber Reinforced Shape Memory Polymer Rebars		5. Report Date December 2024	
		6. Performing Organization Code N/A	
7. Author(s) Guoqiang Li, PhD		8. Performing Organization Report No. LS-23-RP-01	
9. Performing Organization Name and Address Department of Mechanical & Industrial Engineering Louisiana State University S Quad Dr 3261, 3304, Baton Rouge, LA 70808		10. Work Unit No. N/A	
		11. Contract or Grant No. 69A3552348333	
12. Sponsoring Organization Name and Address Transportation Infrastructure Precast Innovation Center (TRANS-IPIC) University of Illinois Urbana-Champaign Civil & Environmental Engineering 205 N Mathews Ave, Urbana, IL 61801 US Department of Transportation Office of Research, Development and Technology (RD&T) 1200 New Jersey Avenue, SE Washington, DC 201590		13. Type of Report and Period Covered Final Report (September 2023 - December 2024)	
		14. Sponsoring Agency Code N/A	
15. Supplementary Notes For additional reports and information visit the TRANS-IPIC website https://trans-ipic.illinois.edu			
16. Abstract The objective of this one-year project was to design, manufacture, and tension program fiber reinforced shape memory polymer (FRSMP) rebars, and test their shape memory effect. Unidirectional glass fiber tow and ultraviolet (UV) curing shape memory polymer with high glass transition temperature will be selected to fabricate the FRSMP rebars. Two types of FRSMP rebars manufactured and tested, one is straight rebar, which will be subjected to tension programming, and the other is curved rebar, which will be programmed by bending. The rebar programming can also be coupled with pre-stressing or post-stressing in pre-cast concrete (PC) construction, so that prior programming can be coupled with construction.			
17. Key Words Precast, Concrete, Transportation, Infrastructure, fiber reinforced shape memory polymer (FRSMP) rebars		18. Distribution Statement No restrictions.	
19. Security Classification (of this report) Unclassified.	20. Security Classification (of this page) Unclassified.	21. No. of Pages 18	22. Price N/A

Disclaimer:

The contents of this report reflect the views of the authors, who are responsible for the facts and the accuracy of the information presented herein. This document is disseminated in the interest of information exchange. The report is funded, partially or entirely, under 69A3552348333 from the U.S. Department of Transportation's University Transportation Centers Program. The U.S. Government assumes no liability for the contents or use thereof.



Transportation Infrastructure Precast Innovation Center (TRANS-IPIC)

University Transportation Center (UTC)

*Design, Manufacturing, and Characterization of Fiber Reinforced Shape
Memory Polymer Rebars
[LS-23-RP-01]*

FINAL REPORT

Submitted by:

*PI: Guoqiang Li, Department of Mechanical & Industrial Engineering,
Louisiana State University, Baton Rouge, LA 70803, E-mail: lquogi1@lsu.edu*

Collaborators / Partners:

None

Submitted to:

TRANS-IPIC UTC
University of Illinois Urbana-Champaign
Urbana, IL

Executive Summary (1-page max):

The objective of this one-year project is to design, manufacture, and tension program fiber reinforced shape memory polymer (FRSMP) rebars and test their shape memory effect. A total of five tasks were proposed. Task 1. Selection of shape memory polymer (SMP) matrix. Task 2. Selection of glass fibers. Task 3. Manufacturing of FRSMP rebars. Task 4. Programming of FRSMP rebars. Task 5. Recovery stress testing.

In Task 1, we selected epoxy resin diglycidyl ether of bisphenol A (DGEBA) cured by isophorone diamine (IPD) to synthesize the shape memory polymer (SMP). Our objective was to achieve a recovery stress higher than 5 MPa. To achieve this objective, we conducted two studies, one was a step-curing approach, and the other was to add nanoclay. Using the step-curing approach, we achieved a recovery stress of about 6.2 MPa for the step-cured SMP. We also used 0.5% by weight nanoclay to further enhance the mechanical and shape memory properties of the SMP. However, the nanocomposite did not yield better results than the pure step-cured SMP. Therefore, we used the pure SMP, but with the new step-curing approach, to prepare FRSMP rebars.

In Task 2, we selected E-glass fiber tows to prepare FRSMP rebars. We investigated two patterns of assembling the fiber tows. One was a straight pattern, with all the filaments along the longitudinal direction, and the other was a braided pattern, with fiber tows braided into cables. We conducted finite element analysis, showing that the braided cables have higher ductility than the plain fiber bundles, which is beneficial for FRSMP rebars because more prestrain can be used to program the FRSMP rebars, and thus, higher recovery stress can be expected. We also used the same number of fiber tows to prepare the two types of cables and did tensile tests until fracture. The test results show that the braided cable has slightly lower tensile strength but higher ductility, which agrees with the modeling results. However, it is found that the resin cannot fully wet through the braided cable during manufacturing. Therefore, we only used the plain fiber bundles to prepare the FRSMP rebars for the remaining tests.

In Task 3, we used the pure SMP, which was step-cured, and the plain fiber bundles, to prepare the FRSMP rebars. Both vacuum assisted resin infusion molding and pultrusion approaches were employed. We used a Teflon tube as the mold. The results show that this approach can produce both straight FRSMP rebars and curved FRSMP rebars, with the plain fiber bundles fully wet through by the SMP matrix.

In Task 4, we first did fracture test of the FRSMP rebars in the glassy state (at room temperature). We then did cold tension programming by setting the programming strain equal to 70% of the fracture strain. However, we found that after several days of viscoelastic springback, only very low tensile strain was fixed, leading to very low recovery stress. Therefore, we also used hot programming at 170 °C for both the straight and curved FRSMP rebars. Again, the programming strain was determined to be 70% of fracture strain at 170 °C.

In Task 5, we conducted a fully constrained stress recovery test of both the hot tensile programmed and cold tensile programmed FRSMP rebars. The average recovery stress was found to be 1.53 MPa for the straight rebars and 0.85 MPa for the curved rebars.

Clearly, this recovery stress is too low to be used in closing wide-opened cracks in the tension zone of reinforced concrete girders. Therefore, although FRSMP has high mechanical strength and corrosion resistance, the idea of using the constrained shape recovery of FRSMP rebars to close wide-opened cracks in the tension zone was not supported by the test results. Further studies should be towards significantly increasing the recovery stress of the SMP matrix, making the fracture strain of the fiber reinforcement compatible with the deformability of the SMP matrix, and improving the manufacturing approach for braided fiber reinforced SMP rebars.

In this project, two graduate students (one with disability) in Mechanical Engineering, one minority female undergraduate student in Biology and Forensic Science, and one postdoc in Mechanical Engineering were involved in the studies.

Table of Contents

Statement of Problem.....	4
2. Research Plan / Tasks.....	4
2.1.1 Task 1-Selection of shape memory polymer (SMP) matrix.....	4
2.1.2 Physical and mechanical properties test.....	6
2.1.3 Hot tensile programming and stress recovery test.....	6
2.2 Task 2-Selection of glass fibers.....	8
2.2.1 Modeling effort.....	8
2.2.2 Fabrication and testing of braided cable and plain control cable.....	10
2.3 Task 3-Manufacturing of FRSMP rebars.....	12
2.4 Task 4 - Programming of FRSMP rebars.....	13
2.4.1 Cold programming of FRSMP rebars.....	14
2.4.2 Hot programming of FRSMP rebars.....	15
2.5 Task 5-Recovery stress testing of FRSMP rebars.....	16
3. Educational outreach activities.....	16
4. Workforce development activities.....	17
5. Technology transfer.....	17
6. Technology transfer actions.....	17
7. Papers that include TRANS-IPIC UTC in the acknowledgments section.....	17
8. Presentations and posters of TRANS-IPIC funded research.....	17
9. Any other events or activities that highlights the work of TRANS-IPIC research that occurred at your university.....	17
10. Any mentions/references to TRANS-IPIC in the news or interviews from your research.....	17
11. References.....	17

TRANS-IPIC Final Report:

1. Statement of Problem

The transportation infrastructure in this nation is deteriorating rapidly. As the world's most developed country, the United States has third-world transportation infrastructure. In the United States, 1 in 5 miles of highways and major roads, and 45,000 bridges, are in poor conditions. The collapse of bridges continuously makes news, with the newest being a bridge collapse in I-95 near Philadelphia. The rapidly deteriorating transportation infrastructure is becoming a barrier instead of a booster to economic development and society wellbeing. Repair, rehabilitation, reinforcement, and reconstruction of our transportation system is becoming a consensus by both parties, as evidenced by the signature "Build Back Better Framework" passed by the legislation in 2021. Within the framework, repairing and rebuilding our roads and bridges with a focus on climate change mitigation, resilience, equity, and safety for all users are key components of the new law. The legislation has reauthorized surface transportation programs for five years and invested \$110 billion in additional funding to repair our roads and bridges and support major, transformational projects. In response to the call for "improving the durability and extending the life of transportation infrastructure" by the Department of Transportation (DoT), a consortium of five universities proposed "Transportation Infrastructure Precast Innovation Center (TRANS-IPIC)" through advancing the technologies used in precast concrete (PC) construction. One of the focus areas of IPIC is to develop fiber reinforced shape memory polymer (FRSMP) rebars, to replace or partially replace conventional steel rebars. In addition to corrosion resistance, the advantage of FRSMP rebars, as compared to conventional steel rebars, persists in their potential ability to serve as both reinforcement during everyday service, and a 'suture' to close cracks and reduce deflection on-demand once they are triggered for constrained shape recovery, enhancing the service life of the PC beams or columns. The objective of this one-year project is to design, manufacture, and tension program fiber reinforced shape memory polymer (FRSMP) rebars and test their shape memory effect.

2. Research Plan / Tasks

A total of five tasks were proposed. Task 1. Selection of shape memory polymer (SMP) matrix. Task 2. Selection of glass fibers. Task 3. Manufacturing of FRSMP rebars. Task 4. Programming of FRSMP rebars. Task 5. Recovery stress testing.

2.1 Task 1-Selection of shape memory polymer (SMP) matrix

In our previous study, we have designed and synthesized a new thermoset shape memory polymer, which demonstrated a record-high recovery stress under compression programming [1]. Therefore, in this project, we selected this polymer, which was an epoxy resin diglycidyl ether of bisphenol A (DGEBA) cured by isophorone diamine (IPD). However, the previous study shows that this polymer has lower tensile fracture strain (6.7%) and lower stabilized recovery stress under tension programming (5 MPa), which is critical for the new application. In order to enhance the fracture strain and recovery stress, we conducted two studies in this project. One is to change the curing condition, and the other is to add nanoclay to the polymer matrix. In the following, we will focus on describing the preparation of the nanocomposite. The curing condition is the same for both the nanocomposite and the pure polymer.

2.1.1 Preparation and curing of the polymer and nanoclay reinforced polymer

In this project, we purchased montmorillonite clay containing 15~35% octadecylamine from Sigma-Aldrich. The epoxy resin was diglycidyl ether of bisphenol A (EPON 826) and the curing agent was isophorone diamine (IPD), which were also purchased from Sigma-Aldrich; see **Figure 1(a)**.

The process of reinforcing the epoxy resin by nanoclay began with determining the amount of the nanoclay required to achieve 0.5% mass fractions of the total resultant mixtures. One gram of the nanoclay was weighed and placed into a round bottle, 3 neck angled flask. Next, 200 mL of high purity solvent N,N-Dimethylformamide (DMF) sourced from EMD Chemicals was introduced to the flask. The solution was then mixed with a mechanical mixer at 330 rpm while the outside of the flask was submerged in an Emerson Branson 8800 CPXH digital ultrasonic bath to further agitate the clay solute. The mixing was limited in duration to 100 minutes to keep the bath water at or below 25 °C and allow it to cool in between cycles. A minimum of two such cycles were conducted for each nanoclay and DMF solution. The flask was then removed from the mixer and the ultrasonic bath while the contents inside the flask were allowed to settle, if any, for 1 h.

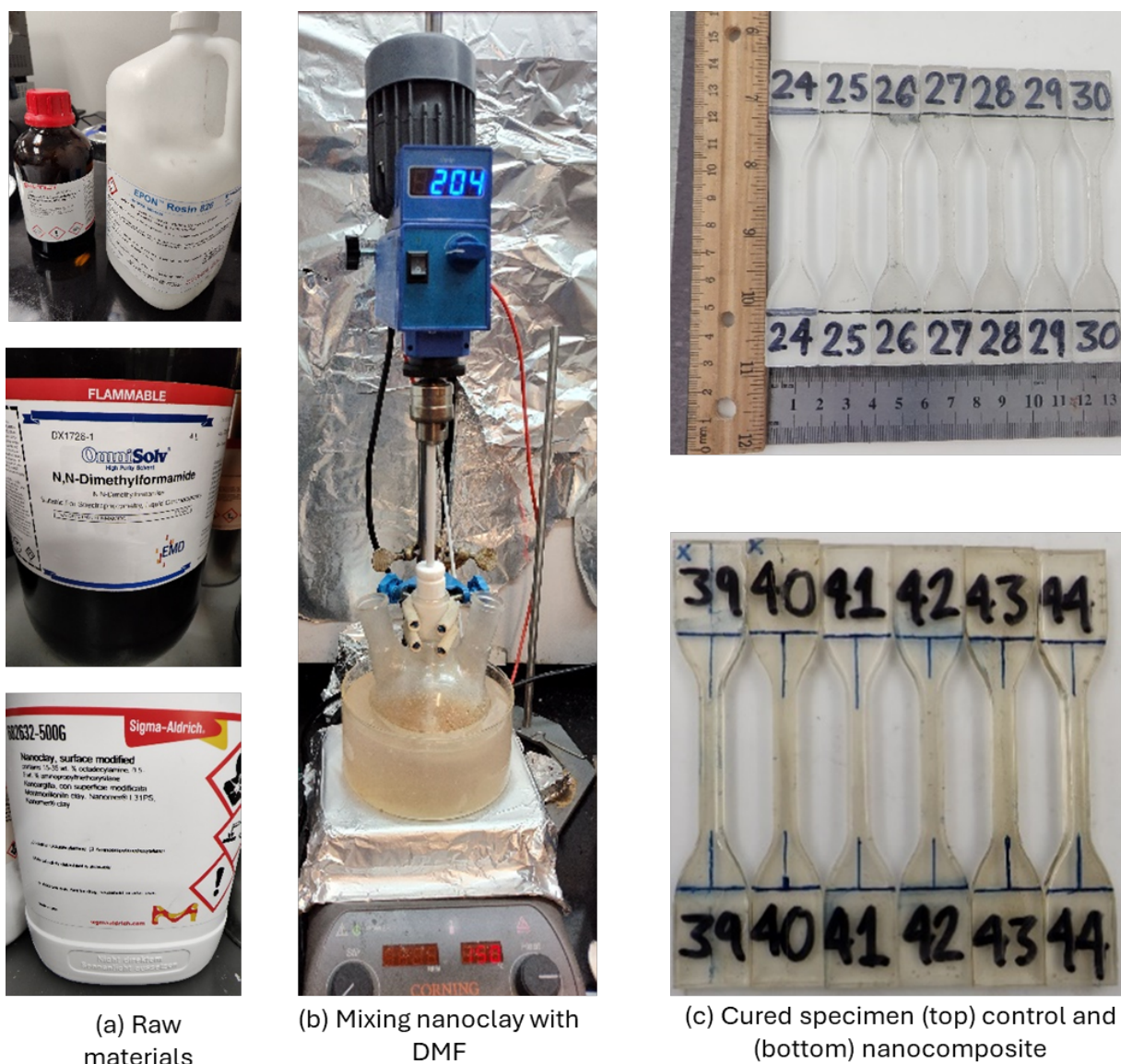


Figure 1. Nanoclay reinforced polymer and pure polymer preparation.

After confirming that the nanoparticles remained completely suspended in the solution, the predetermined amount of the commercial epoxy EPON 826 was heated at 80 °C in a beaker

until liquified. The nanoclay/DMF solution was combined with the epoxy resin in the beaker which was then mixed at 200 rpm at an elevated temperature of 90 °C for 48 h and then 120 °C for 12 h to allow time for the DMF solvent to evaporate out of the solution; see **Figure 1(b)**. Once these preliminary steps were completed, the EPON 826/nanoclay mixture was prepared by the addition of the hardener Isophorone Diamine (IPD, 5-amino-1,3,3-trimethylcyclohexanemethylamine) into the EPON/nanoclay mixture at room temperature in a proper stoichiometric ratio of 23.2 g IPD per every 100 g of epoxy. The mixture was mixed fully at 75 rpm for 5 minutes and then transferred to a mold which was placed in a vacuum chamber for 30 minutes at room temperature to eliminate all air bubbles. The mixture was first cured at 60 °C for 30min, then 100 °C for 1 h, and 150 °C for another 1 h. **Figure 1 (c)** shows some of the prepared dogbone specimens.

2.1.2 Physical and mechanical properties test

The mechanical properties of the control and 0.5% Nanoclay sample groups were tested at the elevated temperature of 170 °C, sufficiently above the glass transition temperature region of the polymer (about 140 °C as determined by an DSC machine; see **Figure 2**). The typical results for the specimens tested until fracture are shown in **Figure 3**.

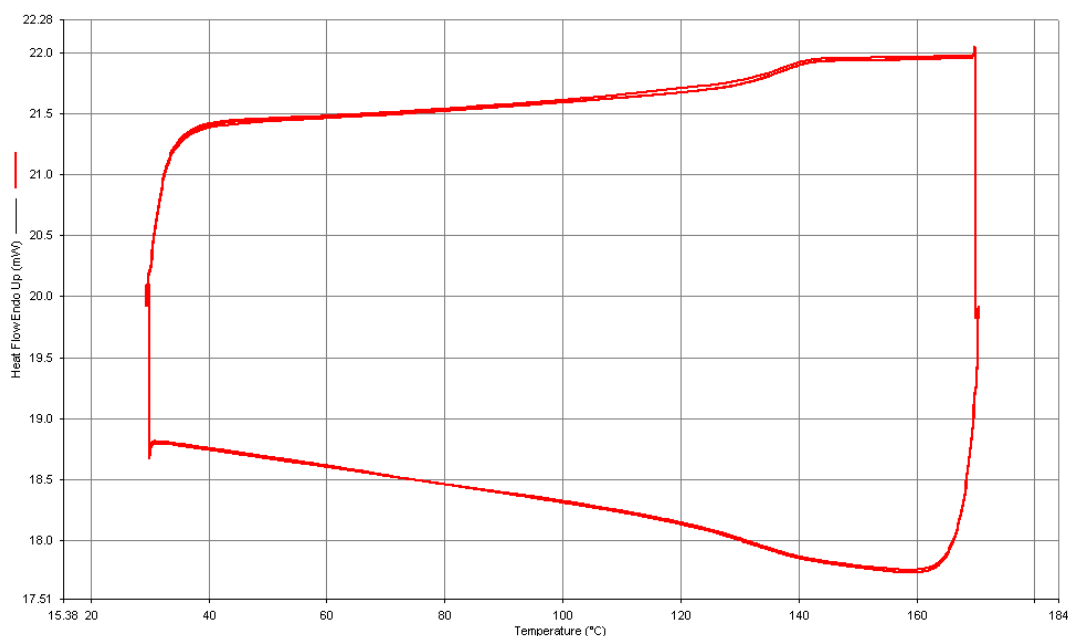


Figure 2. DSC test results of the pure polymer.

From **Figure 3**, it is seen that both the peak stress and the fracture stress of the control specimens were higher than those of the nanocomposite. However, the fracture strain of the nanocomposite is higher than that of the control polymer. The reason for this is likely due to the remaining solvent in the nanocomposite, which served as a plasticizer to the polymer. Clearly, in future studies, action must be taken to fully eliminate the entrapped solvent to display the reinforcement effect of the nanoclay particles.

2.1.3 Hot tensile programming and stress recovery test

We conducted hot programming of the dogbone samples. The test started by preheating the MTS environmental chamber to 170 °C for 1 hour to allow for temperatures and any thermal expansion of the fixtures to stabilize. The specimens were also heated in the chamber for 20 minutes prior to any fracture testing or programming to allow them to effectively transition from

the glassy to rubbery state. Once the temperature stabilized, we opened the door of the chamber and quickly clamped the sample to the MTS machine grips. After about 5 minutes, we applied a tension force at a rate of about 0.5 mm/min. Once the strain reached 70% of the fracture strain for either the control or nanoclay group, the tension was stopped, and the strain was maintained for 30 minutes. After that, we started cooling the specimen while keeping the strain constant. Once the temperature dropped to below the glass transition zone (the glass transition temperature was 140 °C based on our DSC test results), the force was removed, accompanied by slight springback. The shape fixity ratio was 91% for the control group and 87% for the nanoclay group. During the stress recovery tests, we again heated the chamber to 170 °C and stabilized for 1 hour. We then quickly clamped the tension-programmed sample to the grips of the MTS machine, and the MTS machine started to record the force as a function of time while keeping the recovery strain zero. This led to the fully constrained stress recovery test. The tests lasted between 30 minutes and an hour to allow the change of the recovery stress with time to stabilize as the data curve approached a horizontal asymptote signifying a constant value was achieved. The typical recovery stress test results are shown in **Figure 4**.

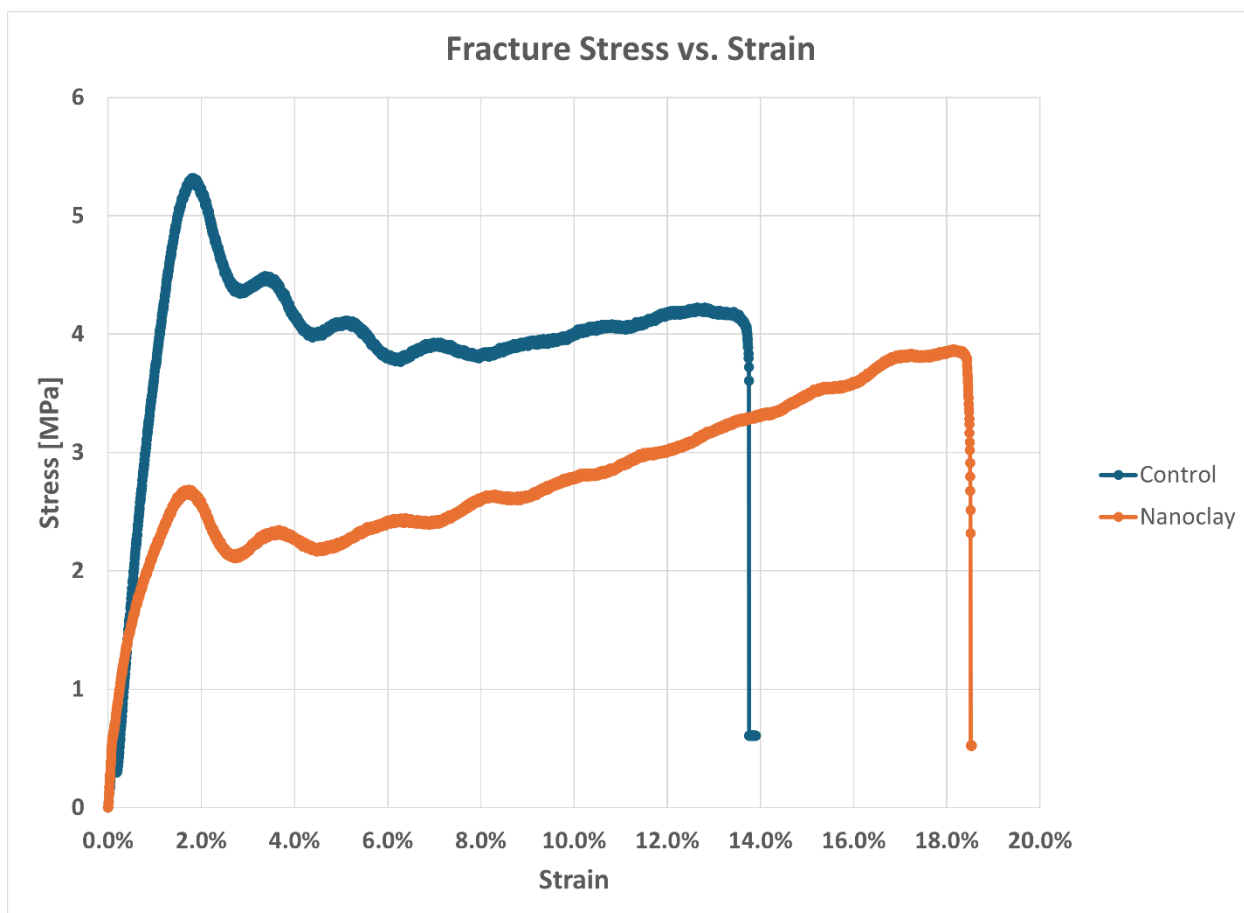


Figure 3. Elevated temperature fracture test results for a typical control and 0.5% nanoclay sample.

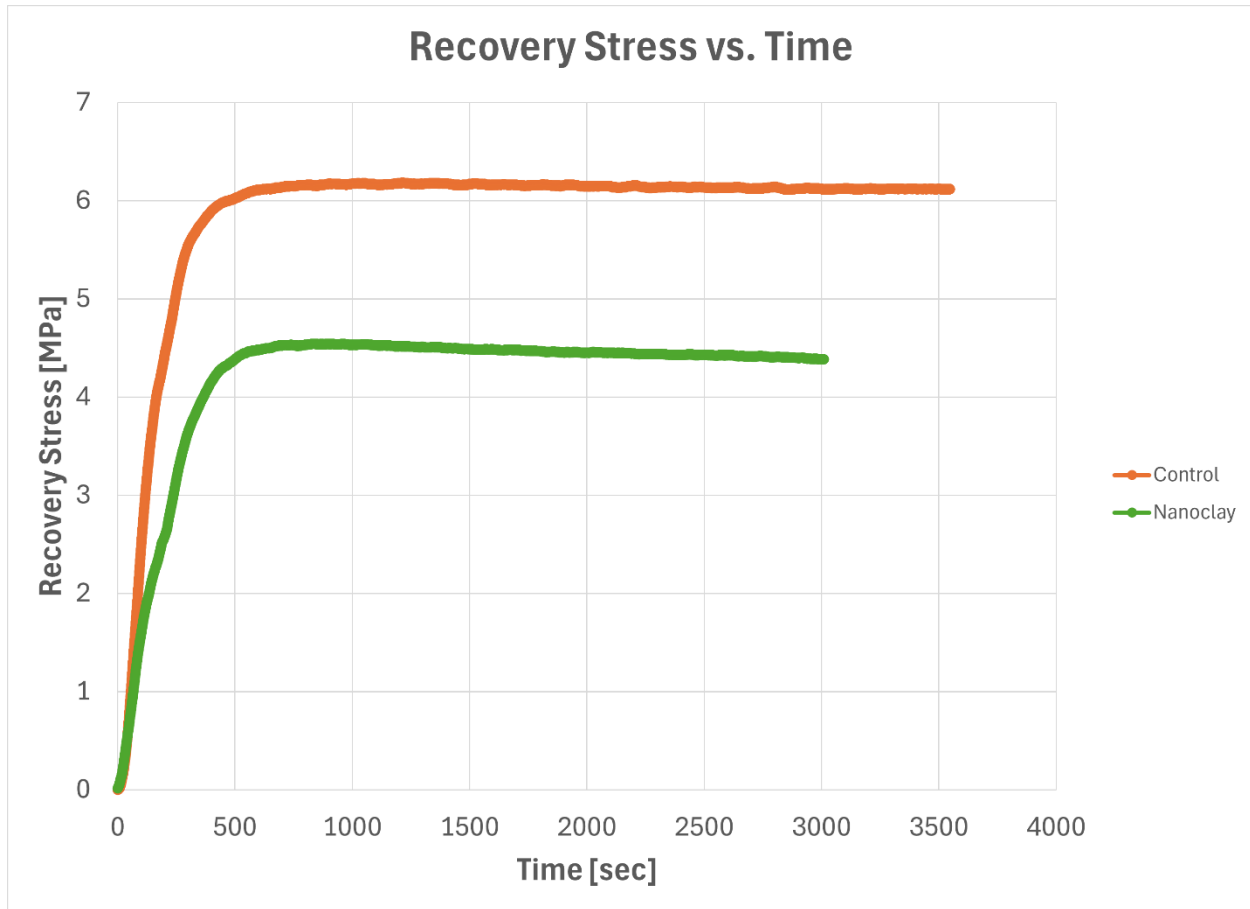


Figure 4. Typical recovery stress vs. time test results for a typical control and 0.5% nanoclay sample.

From **Figure 4**, it is seen that the step-cured polymer has higher recovery stress than that of the nanocomposite. This is consistent with the fracture test. It seems that the solvent was not fully removed from the nanocomposite, leading to lower recovery stress. However, the pure polymer has a recovery stress of about 6.2 MPa, which is higher than that reported previously using a different curing method [1]. Therefore, we used the pure polymer to prepare fiber reinforced polymer rebars in the following Tasks.

2.2 Task 2-Selection of glass fibers

In this project, commercially available E-glass fiber tows purchased from Fibre Glast Development (USA) were selected. The fiber tows can be made into different patterns as reinforcement for the rebar. In this study, we investigated two patterns: one is plain fiber cable by combining several fiber tows so that all the filaments are along the longitudinal direction. The other was braided cable, by braiding several fiber tows into a cable. We conducted both finite element modeling and experimental testing.

2.2.1 Modeling effort

In FR SMP rebars, it is the SMP matrix that has the shape memory effect. In order for the FR SMP rebars to have shape memory effect, more mechanical energy needs to be input to the rebars during tension programming. It is well known that glass fibers have limited deformability,

limiting the amount of deformation that the FRSMP rebars can have. Therefore, the idea is that if the glass fibers tows are braided into different patterns, the braided fiber cables may have higher ductility than that of the plain fiber cable, i.e., the cable is made of straight fiber tows.

As shown in **Figure 5**, we braided three fiber tows into a cable. Modeling a well-laid braided rope involves considering various geometrical factors to accurately represent its structure. The key factors include the diameter of individual strands, number of strands, helix angle, pitch, rope diameter, and braid pattern. To model a well-laid braid rope, it is crucial to consider the diameter of individual strands and the total number of strands used in the braid. Another vital factor is the helix angle and the pitch, or the distance along the rope's length over which a complete helical turn of a strand occurs, which is also an essential geometrical factor that refers to the angle at which the strands are braided around the rope. As an example, we modeled a cable braided by three fiber tows and a cable by plain fiber tows as control, as shown in **Figure 5**. Using the sample boundary conditions, same applied load, same amount of fiber tows, and same material properties, the longitudinal stress and longitudinal displacement are shown in **Figures 6 and 7**, respectively. From **Figure 6**, it is seen that the braided cable has lower longitudinal stress than that of the control plain cable. From **Figure 7**, the braided cable has higher longitudinal displacement than the plain cable. These features are desired for the FRSMP rebars, suggesting more prestrain can be applied during tensile programming so that more energy can be input and be stored in the rebars, and as a result, more recovery stress can be obtained.

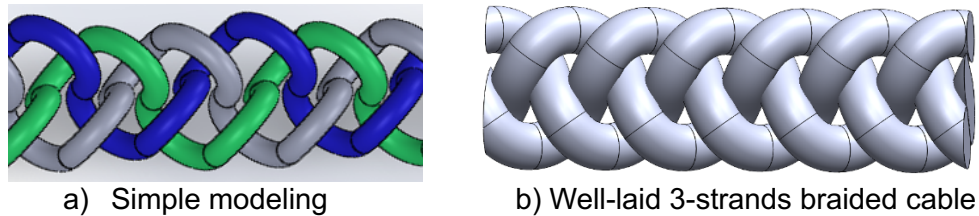


Figure 5. CAD models of braided cables.

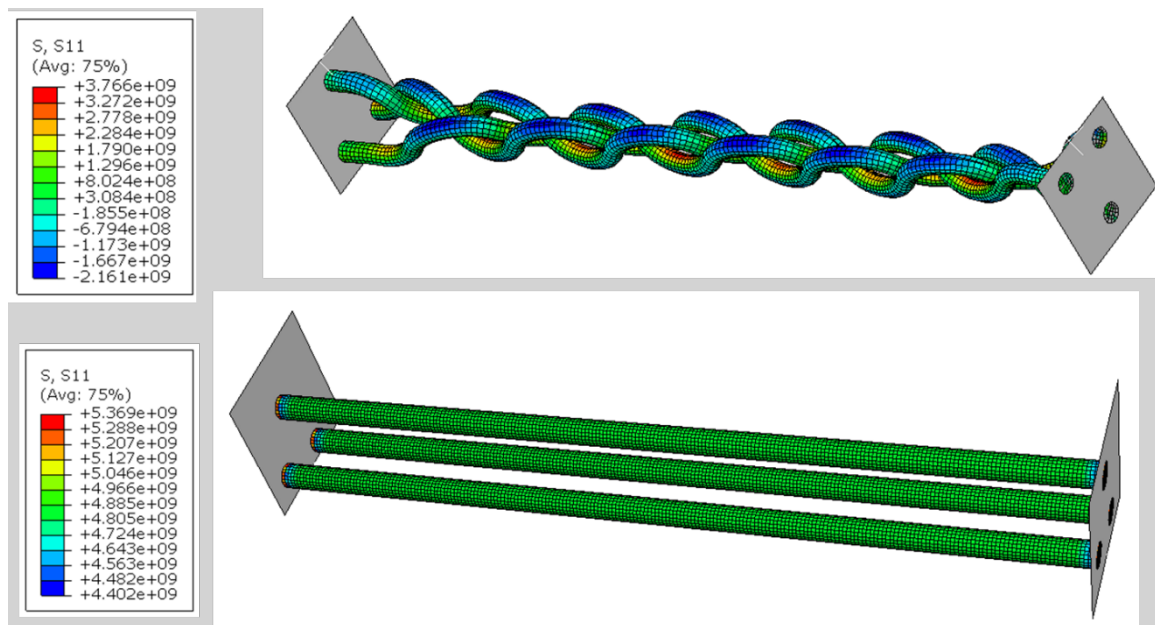


Figure 6. Longitudinal stress distribution in plain and braided cables.

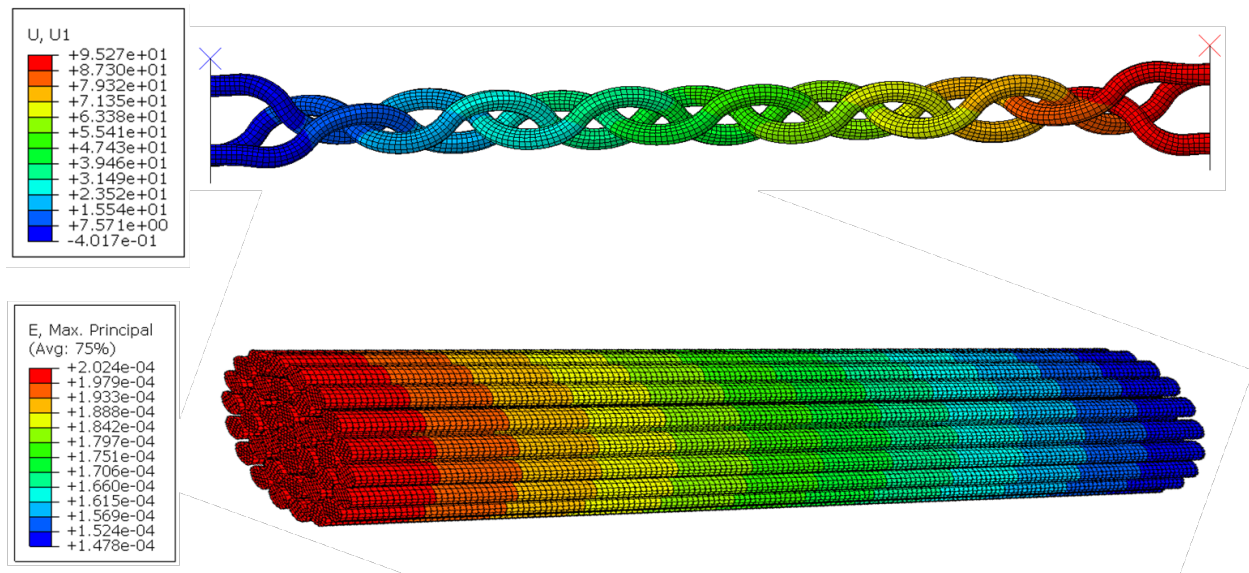


Figure 7. Longitudinal displacement distribution in braided and plain cables.

2.2.2 Fabrication and testing of braided cable and plain control cable

Concurrent with modeling work, we started braiding glass fiber tows into cables, and testing them. In this effort, we first braided three fiber wires into cables. Each wire consisted of six fiber tows. The same number of wires was used to prepare three-wire plain cables as control. We used the SMP to bond the end sections of the cables so that the cable can be clamped by the MTS machine. **Figure 8** shows the uniaxial tensile test results. It is seen that the two types of cables have similar peak load and strain at the peak load. However, it is seen that the braided cable shows a gradual post-peak descending branch, instead of brittle failure in the control cable, suggesting that the braided cable can sustain larger axial tensile strain, which is desired for programming the FRSMP rebars.

We then braided six fiber wires into cables. Each wire consisted of six fiber tows. Therefore, the cable consisted of thirty-six fiber tows. The cables were braided manually. The glass fiber reinforcement was created by first bundling six strands or tows of glass fibers of equal length together for each of the six cords or wires. After anchoring one end of all six cords to a fixed support, the cords were separated into two groups of three, one to the left and the other to the right as seen in Step A in **Figure 9**. The braiding process then began by bringing the leftmost bundle (cord 1) behind all other cords to the right and then weaving it over cord 6, under cord 5, and over cord 4 until finally returning to the left group/side stopping in cord 3's previous position as seen in Step B in **Figure 9**. Next, the rightmost bundle (cord 6) was brought behind all other cords to the left and then woven over cord 2, under cord 3, and over cord 1 after which it finally returned to the right group/side stopping in cord 4's former position as depicted in Step C in **Figure 9**. This process was repeated with the same pattern for the outermost cord alternating between the left and right side until the same initial configuration was obtained with the cords in their original order from 1 to 6. Then, the loose braid was tightened into a compact structure, and the process was continued until the desired length of braided cable was achieved. At the same time, the plain cables made of six straight fiber wires were also prepared manually, as controls. The two end sections of each cable were impregnated with SMP, so that the cables can be clamped by the clamps of the MTS machine. We then conducted uniaxial tension tests of each cable until failure. The typical load versus strain curves are shown in **Figure 10**.

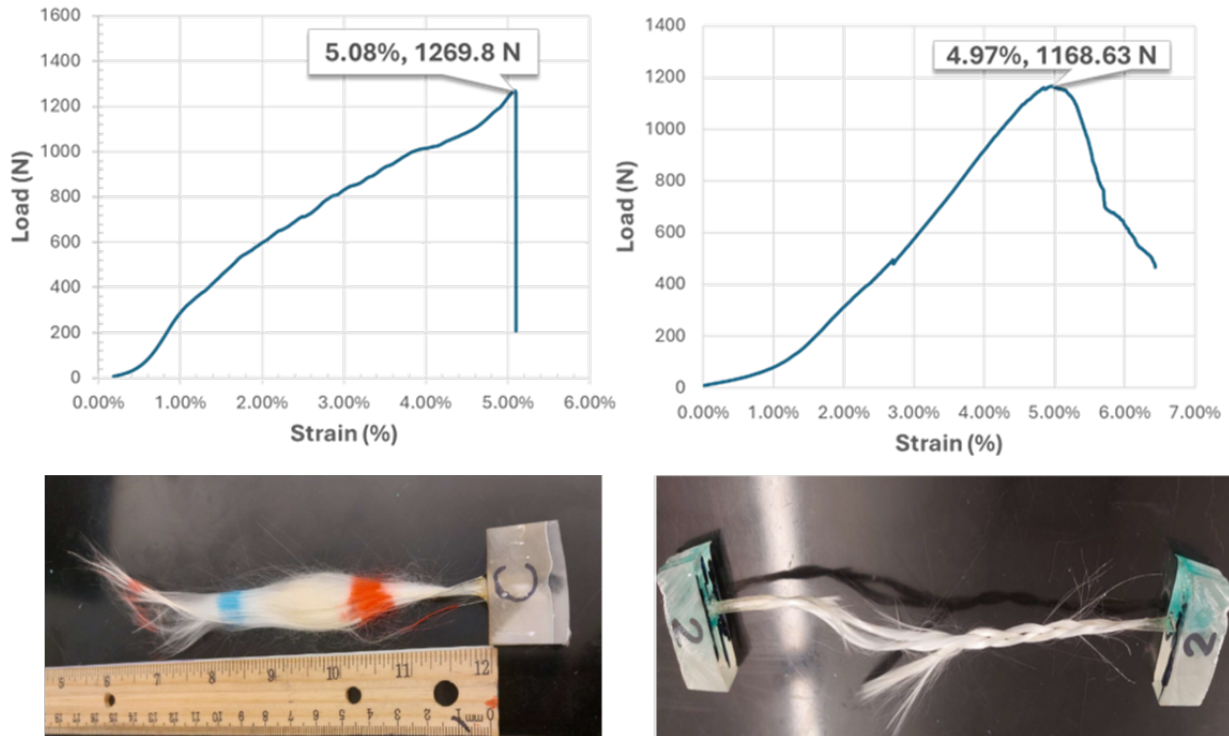


Figure 8. Uniaxial tensile test results (left) control cable and (right) braided cable.

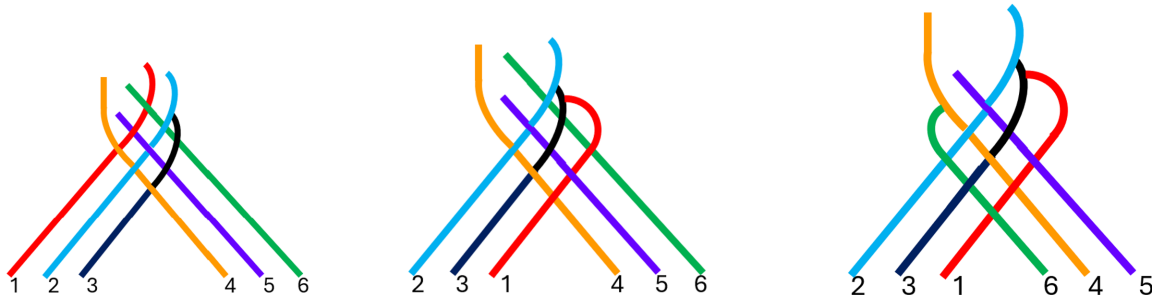


Figure 9. Schematic of preparing the braided cable (from left to right, they are Step A, Step B, and Step C).

From **Figure 10**, it is seen that under the same axial load, the strain of the braided cable is larger than that of the plain cable. This feature is desired because it allows more deformation of the SMP matrix when the FRSMR rebars are tension programmed. As a result, it is expected that the FRSMR rebars with the braided cable reinforcement will have higher energy storage, and higher recovery stress when triggered to have shape recovery, and thus may have the potential to close wider-opened cracks in FRSMR rebar reinforced concrete beams.

The failure modes of the two types of glass fiber cables are shown in **Figure 11**. It is seen that the failure is due to fracture of the fiber tows, at the middle of the gauge length of the cables. The SMP bonded cable ends are in integrity, suggesting that the SMP has very good bonding with the fiber cables. The fiber reinforced SMP section can survive the tensile, shear, and compressive forced applied to it by the clamps of the MTS machine. In other words, the method used to prepare FRSMR rebars, which is a focus of Task 3, is reliable.

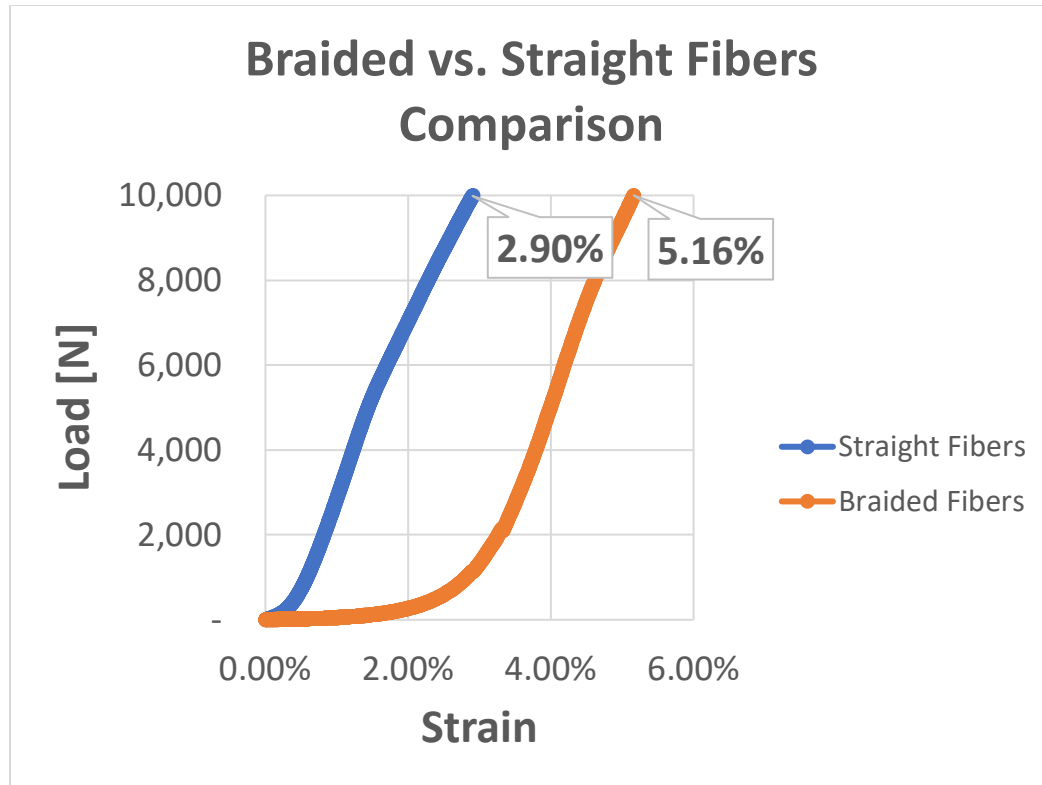


Figure 10. Typical load versus strain test results of braided cable and plain cable.

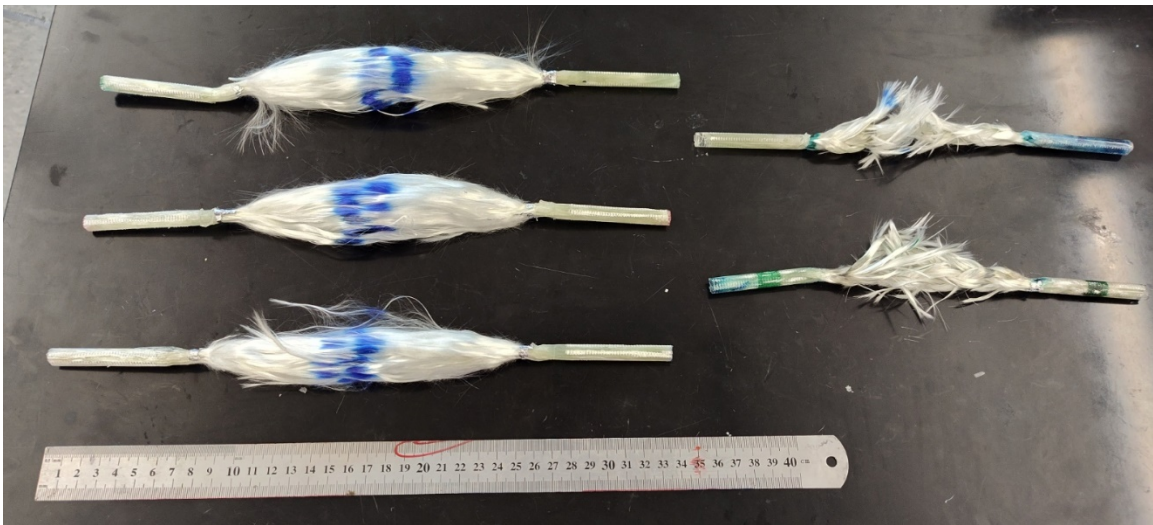


Figure 11. Failure modes of the braided (right) and plain (left) cables after uniaxial tensile tests.

2.3 Task 3-Manufacturing of FRSMP rebars

In this project, we used two manufacturing approaches. We used the pultrusion and vacuum assisted resin infusion molding (VARIM) method to prepare FRSMP rebars. We used 9 mm inner diameter Teflon tubing as the mold; we also used the resin bath which prevented the resin from entering the vacuum pump, and various other supplies including hose clamps, connectors, barbs, and plugs in preparing the clamp sections for the fiber cables. The setup for the VARIM approach is shown in **Figure 12**. In this setup, the shape memory polymer resin was siphoned out of the rectangular aluminum resin bath into the Teflon tubing which contained the

braided fiber cable or plain fiber cable and acted as the mold, giving the rebar its external shape and dimensions. The vacuum pump ensured the fiber was completely infused with resin throughout its length and that voids were minimized. After the fiber core was fully saturated, the tubing containing the composite rebar was disconnected, plugged at both ends, and placed in an oven for curing. However, we found that the VARIM approach did not work well for preparing FRSMP rebars. The reason is that viscosity of the SMP is too high. We also tried to heat it up to reduce the viscosity. However, the working window is too short because high temperature led to partial curing, leading to even higher viscosity. Using diluent also did not work because it cannot be removed from the long rebar within a mold.

Therefore, we also used the classical pultrusion approach to prepare rebars. The straight and curved FRSMP rebars were prepared by first measuring and cutting 75 cm length strands of E-glass fiber per rebar. To achieve a 60% fiber volume fraction, 36 such strands were used per rebar along with a 30 cm long PTFE tube with 9 mm inner diameter. The strands were fed through the tubing, and then the polymer was synthesized through the liquifying, mixing, and vacuum chamber processes. Next, one-half of the fibers in the central section were exposed and submerged into a polymer resin bath as seen in **Figure 13(a) and (b)**. After allowing the fibers to fully soak in the polymer for 15 minutes, the other half of the fibers in the central section were exposed through pultrusion by hand. This cycle was repeated so that both sections were each submerged twice for a total of 30 minutes per side. Then, both ends were trimmed, capped off with silicone plugs, and constricted with hose clamps that were tightened to secure the caps. For curved rebars, the mold was curved manually and clamped to fix the curved shape; see **Figure 13 (b)**. Finally, the rebars were cured in a stepwise manner from 30 °C to 150 °C using increments of 10 °C which were held constant for 5 minutes with the ultimate step involving curing at 150 °C for 1 hour. The circular rebars prepared have an average diameter of about 8.7mm and length of 300 mm. For fracture test and tensile programming test, the average gage length is about 180 mm. The curved rebars were manufactured with a 32.5 cm radius of curvature in their central section.

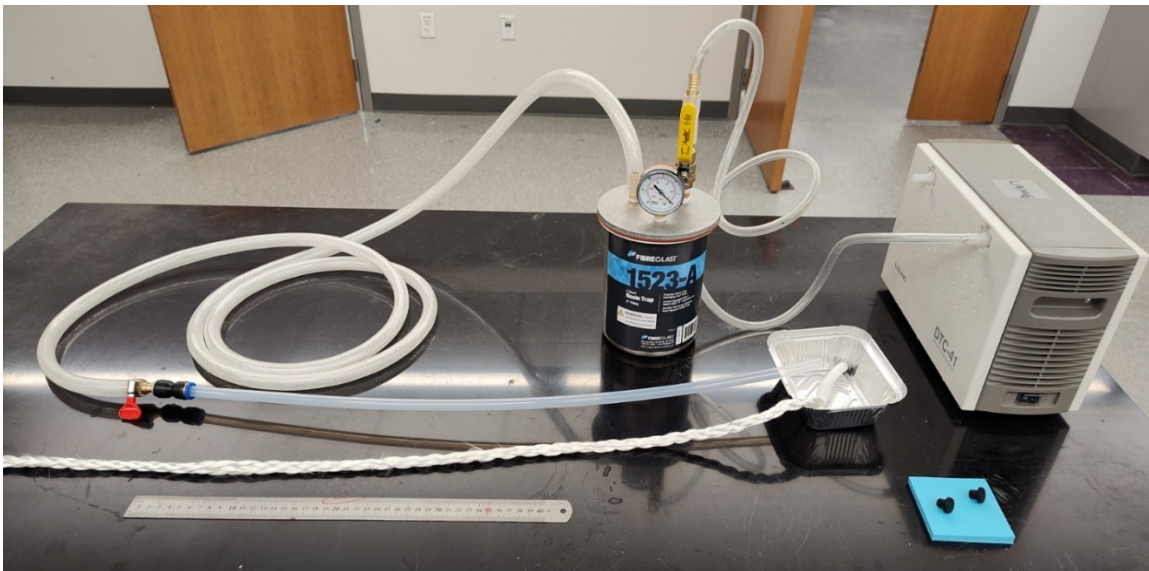


Figure 12. Preliminary rebar fabrication setup per the VARIM approach.

2.4 Task 4 - Programming of FRSMP rebars

In this project, both cold programming and hot programming were utilized to train the FRSMP rebars.

2.4.1 Cold programming of FRSP rebar

The straight and curved rebars were programmed at room temperature by an MTS 810 machine as seen in **Figure 14 (a), (b), and (c)**.

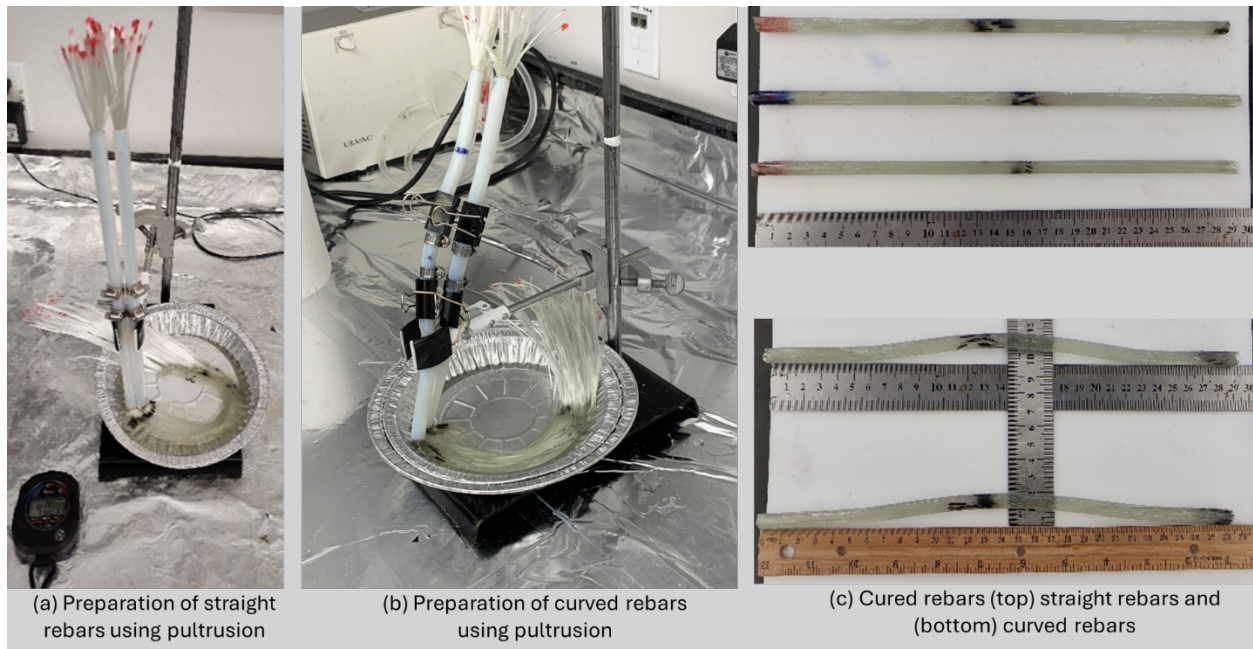


Figure 13. Preparation of FRSP rebars using the pultrusion approach.

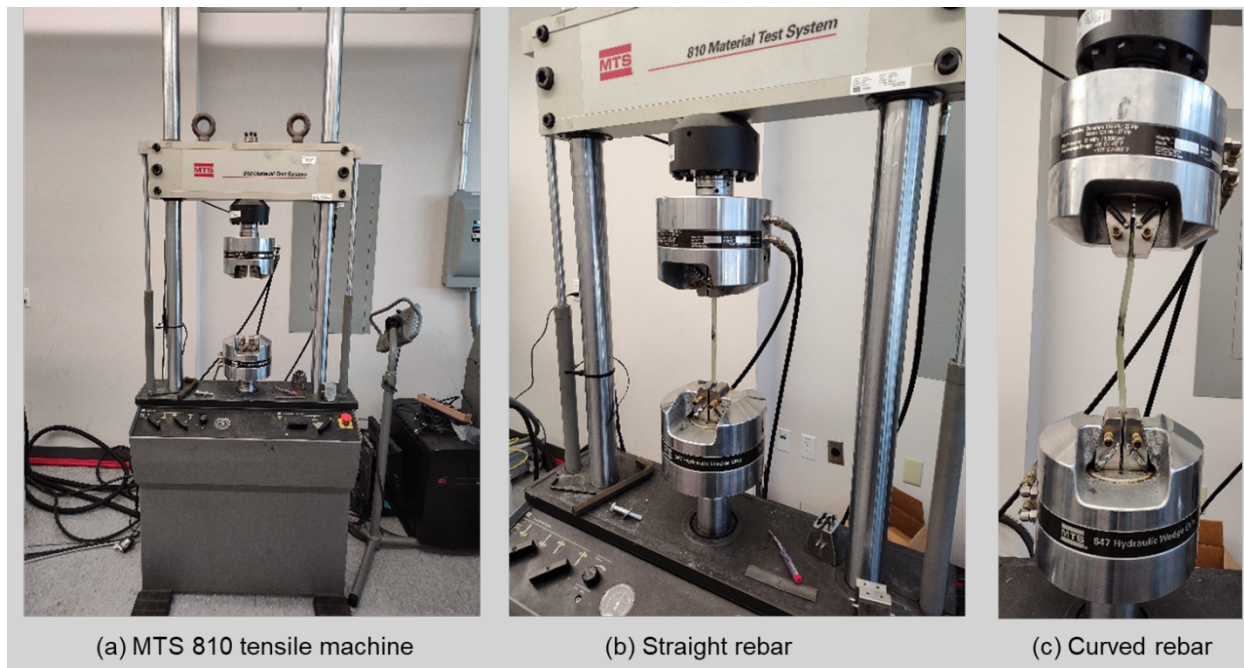


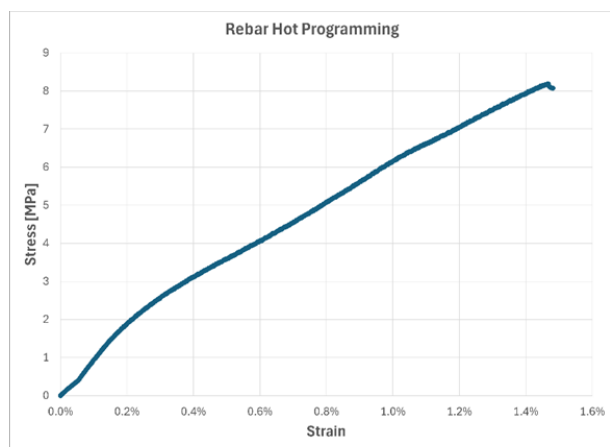
Figure 14. FRSP rebar being cold programmed.

Based on the tensile fracture test conducted at room temperature, the minimum fracture strain of the straight rebars occurred at about 5.0%. Based on the 70% rule and to prevent microcracking from occurring, 3.5% was selected as the programming strain for both the straight and curved rebars. The rebars were tensioned to 3.5% strain at room temperature and were

maintained for 30 minutes. After that the load was removed, accompanied by springback. After several days at the room temperature, the fixed strain is about 1%, due to viscoelastic springback and the compression applied by the fiber reinforcement on the SMP matrix. Therefore, the shape fixity ratio is only about 28.0%, which is much lower than the matrix, which is over 90%. Therefore, it seems that cold tensile programming should be avoided although cold programming is a viable alternative for pure SMP matrix [2].

2.4.2 Hot programming of FRSMP rebars

In order to increase the fixed strain, we also tried to conduct hot programming. However, we encountered difficulties. One is that the height of the standard environmental chamber in our MTS 810 machine is too small to hold our rebars inside. The environmental chamber in our ADMET eXpert 2610 Tabletop 5kN Universal Test System does not have V-shaped jaws to clamp the circular rebars tightly. We used a high glass transition temperature polymer to add tabs to the two ends to the rebars so that the flat ends can be clamped. However, at 170 °C, the polymer tabs softened, and large tensile strains cannot be applied. For hot tensile programming, the following steps were followed: (1) For the hot tensile programming, heat up the chamber to 170 °C first, keep for about 30 minutes, quickly clamp the specimen, and wait for another 30 minutes. (2) After that, tensile programming the specimen to the determined tensile strain, keep it for 30 minutes, and then cool down quickly to room temperature by open the door of the environmental chamber and may also blow cold air to the specimen, and (3) once the temperature is cooled down to room temperature, which is well below the glass transition temperature of the SMP, unload, which may be accompanied by a small springback, completing the hot programming process. **Figure 15 (a)** shows a typical hot tensile programming stress-strain curve, and **Figure 15 (b)** shows the rebars are tabbed by the high temperature polymer. From **Figure 15 (a)**, the programming strain was only about 1.5%, which is very small. One reason for this is that the tabs used were softened during the hot tensile programming test, leading to slipping between the tabs and the grips. This low programming strain suggests that the recovery stress of the rebars may be very low. Because of the small tensile stress during hot tensile programming, the springback upon removing the tensile load is very small, leading to a shape fixity ratio of the rebars above 90%.



(a) Typical hot programming stress-strain curves



(b) Curved (top) and straight (bottom) rebars tabbed with a high temperature polymer

Figure 15. Hot programming of FRSMP rebars.

2.5 Task 5-Recovery stress testing of FR SMP rebars

For stress recovery tests, we heated the environmental chamber to 170 °C first, kept for 1 h, and then quickly clamped the programmed specimens. After that, we observed the stress change over time. We conducted the stress recovery test until the recovery stress was stabilized with time. Typical recovery stress with time curves for both hot and cold programmed FR SMP rebars are shown in **Figure 16 (a) and (b)**, respectively.

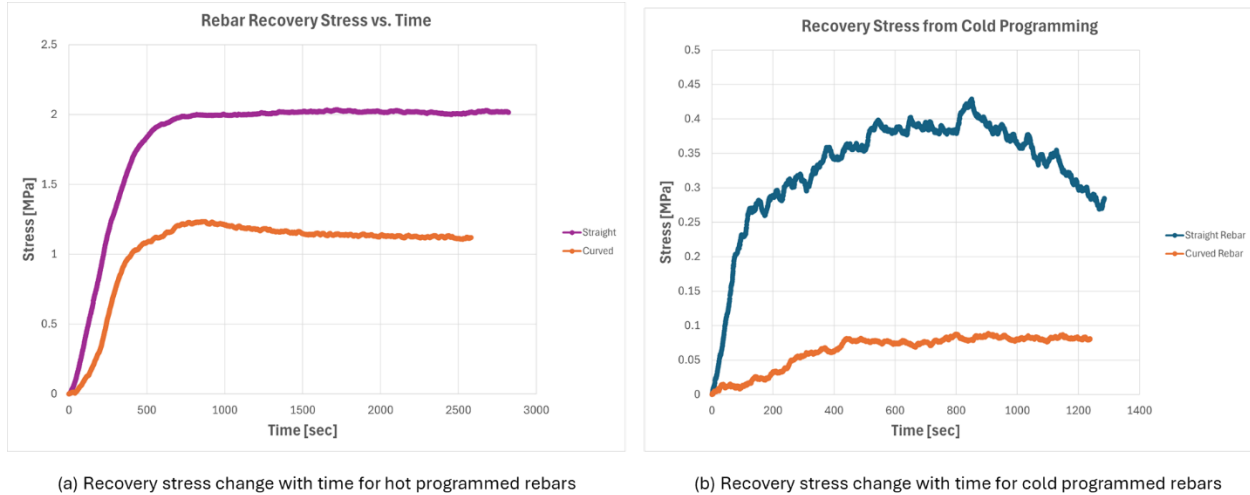


Figure 16. Typical recovery stress change with time for hot programmed straight and curved FR SMP rebars.

From **Figure 16 (a)**, it is seen that after about 30 minutes of testing, the recovery stress for both types of rebars stabilized. The recovery stress for the straight rebar is about 2 MPa, and it is about 1.2 MPa for the curved rebar. These recovery stress results are much lower than the pure SMP matrix, which is about 6.2 MPa. The key persists in the programming strain. For the SMP matrix, it can be tensile programmed over 10% strain, while it is only 1.5% for the hot programmed rebar. We would like to emphasize that the lower programming strain, as discussed in Task 4, is partially due to the inability for us to find a suitable MTS machine to apply the desired tensile strain at 170 °C. We anticipate that the recovery stress should be higher if larger tensile programming strain can be applied to the rebars. We also conducted stress recovery test for cold programmed FR SMP rebars, as shown in **Figure 16 (b)**. As discussed before, because of the extremely low programming strain stored in the rebar, the recovery stress is so small that it can be neglected. Therefore, for this type of FR SMP rebars, we suggest that cold programming be avoided.

3. Educational outreach activities

During this project period, Dr. Guoqiang Li presented “Fiber Reinforced Shape Memory Polymer Rebars” in two seminars:

Seminar 1:

TRANS-IPIC Workshop
Chicago
April 22, 2024.

Seminar 2:

TRANS-IPIC Monthly Seminar
Online through Zoom

4. **Workforce development activities**
None.
5. **Technology transfer**
None.
6. **Technology transfer actions**
None.
7. **Papers that include TRANS-IPIC UTC in the acknowledgments section**
None.
8. **Presentations and posters of TRANS-IPIC funded research**
None.
9. **Any other events or activities that highlights the work of TRANS-IPIC research that occurred at your university**
None.
10. **Any mentions/references to TRANS-IPIC in the news or interviews from your research**
None.
11. **References:**
 - [1] J. Fan and G. Li. High Enthalpy Storage Thermoset Network with Giant Stress and Energy Output in Rubbery State. Nature Communications, Vol. 9, No. 1, paper 642, (2018).
 - [2] G. Li and W. Xu. Thermomechanical Behavior of Thermoset Shape Memory Polymer Programmed by Cold-Compression: Testing and Constitutive Modeling. Journal of the Mechanics and Physics of Solids, Vol. 59, No. 6, pp. 1231–1250, (2011).